The Importance of Protein-Protein Interactions on the pH-Induced Conformational Changes of Bovine Serum Albumin: A Small-Angle X-Ray Scattering Study

Leandro R. S. Barbosa,[†*] Maria Grazia Ortore,[‡] Francesco Spinozzi,[‡] Paolo Mariani,[‡] Sigrid Bernstorff,[§] and Rosangela Itri[†]

[†]Instituto de Física da Universidade de São Paulo, São Paulo, Brazil; [‡]Dipartimento di Scienze Alimentari, Agro-Ingegneristiche, Fisiche, Economico-Agrarie e del Territorio, Sezione Scienze Fisiche, Università Politecnica delle Marche, and Consorzio Nazionale Interuniversitario per le Scienze Fisiche della Materia, Ancona, Italy; and [§]Sincrotrone Trieste, Basovizza, Trieste, Italy

ABSTRACT The combined effects of concentration and pH on the conformational states of bovine serum albumin (BSA) are investigated by small-angle x-ray scattering. Serum albumins, at physiological conditions, are found at concentrations of ~35–45 mg/mL (42 mg/mL in the case of humans). In this work, BSA at three different concentrations (10, 25, and 50 mg/mL) and pH values (2.0–9.0) have been studied. Data were analyzed by means of the Global Fitting procedure, with the protein form factor calculated from human serum albumin (HSA) crystallographic structure and the interference function described, considering repulsive and attractive interaction potentials within a random phase approximation. Small-angle x-ray scattering data show that BSA maintains its native state from pH 4.0 up to 9.0 at all investigated concentrations. A pH-dependence of the absolute net protein charge is shown and the charge number per BSA is quantified to 10(2), 8(1), 13(2), 20(2), and 26(2) for pH values 4.0, 5.4, 7.0, 8.0, and 9.0, respectively. The attractive potential diminishes as BSA concentration increases. The coexistence of monomers and dimers is observed at 50 mg/mL and pH 5.4, near the BSA isoelectric point. Samples at pH 2.0 show a different behavior, because BSA overall shape changes as a function of concentration. At 10 mg/mL, BSA is partially unfolded and a strong repulsive protein-protein interaction occurs due to the high amount of exposed charge. At 25 and 50 mg/mL, BSA undergoes some refolding, which likely results in a molten-globule state. This work concludes by confirming that the protein concentration plays an important role on the pH-unfolded BSA state, due to a delicate compromise between interaction forces and crowding effects.

INTRODUCTION

The study of protein-protein interaction and its behavior in intermediate and high concentrated solutions have received increasing attention in the last decades. It is not rare to find high protein concentrations in physiological and natural conditions. Hemoglobin, for example, is found in erythrocytes at concentrations that can exceed 300 mg/mL (1). For the case of Hemoglobin, the contribution of nonideality to the activity of the protein in salt solution was shown to increase rapidly with increasing protein concentration (2). But protein interactions and further aggregation processes are also very important in understanding Alzheimer's, Kreutzfeld-Jacob, and Parkinsonian-type diseases, which are caused by either protein or peptide association phenomena (3), or eyes lens transparency, which is caused by the short-range order of crystalline proteins (4,5).

Serum albumin is probably one of the most studied models of globular proteins. It is synthesized by the liver in mammals and has a half-life in the circulatory system of ~19 days. Its concentration varies from 35 up to 55 mg/mL in the blood plasma (6). It corresponds to the most abundant protein in blood plasma, accounting for ~60% of the total number of globular proteins (6–8). Serum albumin function is associated with the binding and transport of several small molecules such as fatty acids, dyes, metals, and amino acids, as well as pharmaceutical compounds (6,7,9). Bovine serum albumin (BSA) is constituted by 585 amino acid residues, including 35 Cysteines (17 disulfide bridges), which confer a relatively strong stability to the protein (6,7). Its secondary structure is constituted by 67% α-helix and its isoelectric point (pI) is reported on a pH range from 4.8 to 5.6 (6,10,11).

The crystallographic structure of BSA has not yet been resolved. Because it shares >75% of identity on the primary structure with human serum albumin (HSA) (6) (whose crystallographic structure is known (7)), their structures are considered to be similar (12,13).

There is a large amount of research dealing with BSA at different conditions. In particular, it was previously reported that BSA has different pH-dependent conformations in the diluted regime up to 3 mg/mL (6,14). The normal (or N) form is predominant from pH 4.5 to 7.0. Between pH 4.5 and 4.0, a Normal–Fast (N–F; the F, or Fast form, designates fast-migrating) transition occurs and the F form is abruptly produced upon lowering the pH to values <4.0. At pH <3.5, the expanded (E) form appears. The N–F transition involves a decrease in the content of ordered (secondary) structure. The albumin macromolecule in the N-form is globular, whereas it becomes partly opened in the F-state (6). Interestingly, it was evidenced that HSA undergoes a transition to a molten-globule conformation at pH 2.0 (15); generally the molten globule states are characterized

Submitted May 27, 2009, and accepted for publication September 29, 2009.

*Correspondence: lbarbosa@if.usp.br

Editor: Doug Barrick.

0006-3495/10/01/0147/11 $2.00

doi: 10.1016/j.bpj.2009.09.056

by an abundant secondary structure and a globular structure (16). In addition, another conformational transition takes place between pH 8.0 and 9.0, which is called basic transition (or N–B transition) (6,17). In such case, BSA apparently loses some of its rigidity, likely affecting the protein amino-terminal region (6), and the macromolecule has a small increase in its radius (6). In these studies, however, small attention has been paid on the effect of protein concentration on such transitions.

Despite a large amount of research that had been done on the physico-chemical properties of BSA at different conditions ((18), and references therein), to our knowledge, no systematic study had been performed that focuses on how the pH affects the BSA tertiary structure when the macromolecule is in large amount in the solution. In this article, therefore, we studied BSA at three different concentrations (10, 25, and 50 mg/mL), close to those found in the blood plasma (6), and at different pH values (2.0, 4.0, 5.4, 7.0, 8.0, and 9.0), by means of the small-angle x-ray scattering (SAXS) technique. Under such conditions the protein presents different net charges, and analysis of relationships among the conformational state, the protein concentration, and the protein-protein interaction becomes possible. Data have been analyzed by the Global Fit procedure (GENFIT software (19–21)), which allows the analysis of several scattering curves simultaneously. All results confirm that the protein concentration plays an important role on the pH-unfolded BSA state, due to a delicate compromise between interaction forces and excluded volume effects.

MATERIALS AND METHODS

Materials, sample preparation, and information about SAXS experiments can be found in the Supporting Material.

THEORY

Small angle x-ray scattering

Globular proteins in solution

The scattering intensity from a set of proteins randomly distributed is given by (22,23)

$$I(q) = \gamma n_p P(q) S_M(q), \tag{1}$$

where γ is a calibration factor and n_p corresponds to the protein number density (calculated as 9.1×10^{-8}, 2.3×10^{-7}, and 4.6×10^{-7} Å^{-3}) from the studied protein concentration (10, 25, and 50 mg/mL, respectively). $P(q) = \langle F^2(\boldsymbol{q})\rangle$ is the orientational average of the squared scattering amplitude of the protein, known as form factor, and $S_M(q) = 1+\{\langle F(\boldsymbol{q})\rangle^2/P(q)\}(S(q)-1)$ is the so-called measured structure factor, related to the interparticle interference function $S(q)$ as well as to $P(q)$. We have checked through test calculations that for globular protein states, in the investigated q range, the differences between $S_M(q)$ and $S(q)$ are $< \pm 1\%$, confirming that the rather standard approach of using $S(q)$ in the Eq. 1 instead of $S_M(q)$ is acceptable. In this article, we make use of two different approaches to calculate $P(q) = \langle F^2(\boldsymbol{q})\rangle$ and $\langle F(\boldsymbol{q})\rangle^2$ functions of native BSA. The first approach deals with Monte Carlo simulations, as previously described (20,24,25), using the protein crystallographic structure (in our case, PDB entry 1N5U (26) for HSA in the protein data bank site). The second approach describes the form factor by considering that the protein can be modeled as a two-density level ellipsoid (27). It is important to mention that the hydration shell in both methodologies is taken into account, and its thickness is fixed at 3 Å with an electron density higher than the bulk water electron density (see (28)).

The value $S(q)$ can be calculated analytically (or numerically) for globular proteins by adopting specific closure relations (29). Here we make use of the random phase approximation, which is applicable to moderately charged systems (30,31). The interacting potential is treated as a perturbation of the reference potential (in our case the Hard-Sphere potential) whose corresponding structure factor, $S_0(q)$, is given by Hansen and McDonald (29). The correct protein-protein interaction potential is a matter of debate in the literature (18,31,32). As proteins generally do not adopt simple geometrical shapes, it is difficult to describe their exact interaction potential. Nevertheless, in the literature, there are some potentials that have been widely tested, and had reproduced protein-protein interaction potential satisfactory. Here we use the potential described by Narayanan and Liu (31), which combines an electrostatic screened Coulomb potential and an attractive Yukawa-like potential. This latter potential must be considered as an effective one, since it can take into account such distinct contributions as van der Waals, osmotic, and depletion potentials, among others (33,34). By doing so, the protein-protein interaction potential, $V_{pp}(r)$, can be written as (31)

$$V_{pp}(r) = V_{HS}(r) + V_C(r) + V_Y(r), \tag{2}$$

where $V_{HS}(r)$ is the hard sphere potential,

$$V_{HS}(r) = \begin{cases} \infty \text{ for } r < \sigma_{eff} \\ 0 \text{ for } r \geq \sigma_{eff} \end{cases}, \tag{3}$$

with σ_{eff} as the sphere effective diameter, and

$$V_C(r) = \frac{Z^2 e^2}{\varepsilon\left(1 + (1/2)k\sigma_{eff}\right)^2} \frac{e^{-(k(r-\sigma_{eff}))}}{r}, \tag{4}$$

where

$$k^2 = \frac{8\pi e^2 N_A I}{\varepsilon\, k_B T}$$

is the square of inverse Debye screening length, Z is the net protein charge, e is the fundamental electron charge, ε is the dielectric constant of the solvent, N_A is Avogadro's number,

and I is the total ionic strength determined from both protein counterions, $I_c = (1/2)n_p|Z|$, and added salts, I_s (24). The values of I_s were calculated considering the dissociation constant of each component of the buffer (amounting to 27 mM at pHs 4.0 and 5.4; and to 29 mM, 32 mM, and 36 mM, at pHs 7.0, 8.0, and 9.0, respectively; k_B is the Boltzmann constant and T the temperature. The attractive Yukawa potential is

$$V_Y(r) = -J\left(\frac{\sigma_{eff}}{r}\right)e^{\frac{-(r-\sigma_{eff})}{d}}, \quad (5)$$

where J and d correspond to the potential depth at contact (i.e., $r = \sigma_{eff}$) and the range of the attractive potential, respectively.

Partially unfolded interacting proteins in solution

It is well known that proteins during the unfolding process can reach some intermediate states in which their conformation is neither native nor completely unfolded. Previously, some of us have successfully applied the wormlike polymers approach (35,36) to describe the SAXS curves of partially unfolded cytochrome *c* (37). Here, we make use of the same approach to model $P(q)$, which supposes that the partially unfolded protein can be represented by identical attached cylinders. The fitting parameters are the contour length L and the Kuhn length b, representing the protein maximum extension and each cylinder length, respectively. Moreover, the cylinder cross-section radius R is also a fitting parameter to take the excluded volume effect into account (see (35,37) for further details). In addition, a crucial problem resides in defining the protein-protein interaction potential, because such a potential is certainly not spherically symmetric. As far as we know, this description is still lacking in the literature due to the problem's complexity. Therefore, we apply here a combination of a spherically symmetric interacting potential (Eqs. 2–5) with a semiflexible form factor as a rough trial to describe the SAXS curves of the partially unfolded BSA. However, such an approximation does fail to fit the scattering of unfolded proteins. This point will be better discussed further into the text.

The global fitting procedure

As mentioned earlier, the Global Fit procedure (GENFIT software (19)) allows the analysis of several scattering curves concomitantly (20,21,38). In our case, the protein electron density was fixed at 0.4235 $e/Å^3$, obtained from the protein sequence, and kept constant during the χ^2 minimization. The protein volume, calculated from the HSA crystallographic structure, and the protein effective diameter (σ_{eff}) equal to 92(2) $\times$ 10^3 $Å^3$ and 66(3) Å, respectively, were allowed to vary within a narrow range. The range of the attractive potential, d, was considered to be ~10% of σ_{eff} as proposed by Ortore et al. (39). At each pH, both parameters, σ_{eff} and d, resulted as protein concentration-independent, as did the absolute value of the net protein charge ($|Z|$) (Table 1). The strength of the attractive potential (J), however, depends on both pH and concentration values. The best solution is then obtained by minimizing the reduced χ^2 (20,21,24), in a simulating annealing process (40). By doing so, a γ-value of 3.6(2) $\times$ 10^{-8} was obtained for the whole set of SAXS curves, which corresponds to the common unknown instrumental factor (Eq. 1).

RESULTS AND DISCUSSION

Fig. 1 shows the SAXS curves normalized by the BSA concentration (10, 25, and 50 mg/mL at pHs 2.0, 4.0, 5.4, 7.0, 8.0, and 9.0). The scattering profiles for $q \geq 0.06$ $Å^{-1}$ are quite similar for BSA at pH 4.0–9.0 regardless of the protein concentration. In the low q range ($q < 0.06$ $Å^{-1}$), and at pH 4.0–9.0, a decrease in the normalized SAXS intensities is observed as the concentration increases. Such an effect is due to protein-protein interactions (32,41), which are more noticeable at increasing protein concentrations. In addition, at pH 4.0, 10 mg/mL, one can notice an excess of intensity at low q values, as compared to that observed for the protein at higher pH values. This effect can be due either to the presence of small aggregates in solution or to the appearance of a short-range attractive potential between the proteins (32). Nevertheless, one should notice that the SAXS intensities for low q values obtained at pH 4.0 for higher BSA concentrations (25 and 50 mg/mL) are lower than that of 10 mg/mL BSA at the same pH. This indicates that an effective repulsive protein-protein interaction should take place over the SAXS curve.

Regarding pH 2.0, the normalized SAXS intensities are rather different from those obtained for higher pH values. First of all, one should notice the presence of a peak at

TABLE 1 Fitting parameters obtained by using the global fitting procedure to the systems composed of BSA, 10, 25, and 50 mg/mL, from pH 4.0 to 9.0

pH	4.0			5.4			7.0			8.0			9.0		
[BSA] (mg/mL)	10	25	50	10	25	50	10	25	50	10	25	50	10	25	50
J (k_BT)	28(3)	10(2)	5(1)	13(2)	7(1)	4(1)	20(2)	10(2)	2.0(4)	23(3)	12(2)	6(1)	26(2)	14(2)	8(1)
d (Å)		6.4(6)			3.5(4)			5.0(5)			6.4(6)			6.4(6)	
σ_{eff} (Å)		64(3)			70(4)			67(4)			64(3)			64(3)	
$\|Z\|$ (e)		10(2)			8(1)	13(2)		13(2)			20(2)			26(2)	

The brackets denote concentration; J and d are the attractive potential depth and the potential range, respectively; $|Z|$ is the absolute value of the net protein charge; and σ_{eff} is the BSA effective diameter.

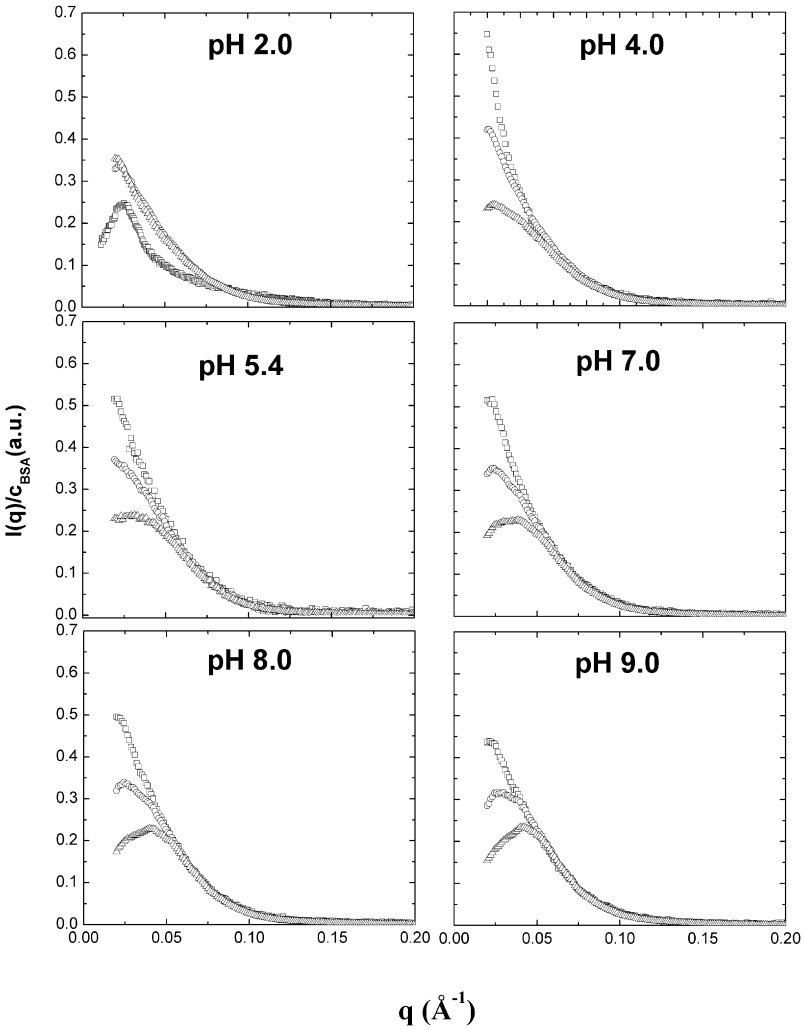

FIGURE 1 SAXS intensities normalized by BSA concentration at $c_{BSA} = 10$ (*squares*), 25 (*circles*), and 50 mg/mL (*triangles*) at the pH indicated.

$q \approx 0.025$ Å^{-1} in the curve observed for 10 mg/mL. Such a strong and well-defined peak was not present in any other pH at this concentration. Furthermore, the experimental data in the Kratky representation ($I(q)q^2$ vs. q, see the Supporting Material) show a plateau for large q values at pH 2.0 and 10 mg/mL, characteristic of unfolded proteins, in contrast to a bell-like curve, typical for globular proteins, for other pHs and concentrations (Fig. S1 in the Supporting Material). Kumar et al. (15) showed that HSA can exist as a molten-globule state at pH 2.0. This possibility will be checked in the SAXS data analysis, as follows.

We now proceed with the data analysis focusing our attention on the systems at pH 4.0–9.0, by means of GENFIT. It should be stressed that, due to protein-protein interaction, $I(q)$ is not described by an exponential function at low q values (known as the Guinier region (22)). Such a fact precludes any extraction of the protein radius of gyration directly from the scattering curves in an independent manner. Indeed, $I(q)$ carries both the influence of the protein form factor $P(q)$ and the interprotein interaction $S(q)$ (Eq. 1), so both have to be evaluated simultaneously.

BSA at pH 4.0 up to 9.0

One of the main difficulties in SAXS data analysis of proteins in solution is to choose which protein form factor, $P(q)$ (Eq. 1), should be used. For instance, in the case of BSA, the protein shape is most commonly treated as effective ellipsoids (which could be either prolate (42–44) or oblate (18)). In some cases, BSA can be represented as a combination of three or six spheres (45), where the sphere represents each domain or subdomain of BSA, respectively. Ferrer et al. (12) demonstrated that BSA can also be represented as a solid equilateral triangular prism (heart-shaped). Here, we used HSA crystallographic structure to calculate the protein form factor, as BSA does not yet have its crystallographic structure determined. To start, we successfully applied the $P(q)$ function generated from HSA crystallographic structure to reproduce the experimental data of BSA (10 mg/mL) at pH 5.4, near its pI (Fig. S2), where there is a subtle influence of the $S(q)$ function over the SAXS curve (Fig. 1).

Therefore, such a form factor was used in the analysis of the systems at pH 4.0, 5.4, 7.0, 8.0, and 9.0 (with 10, 25,

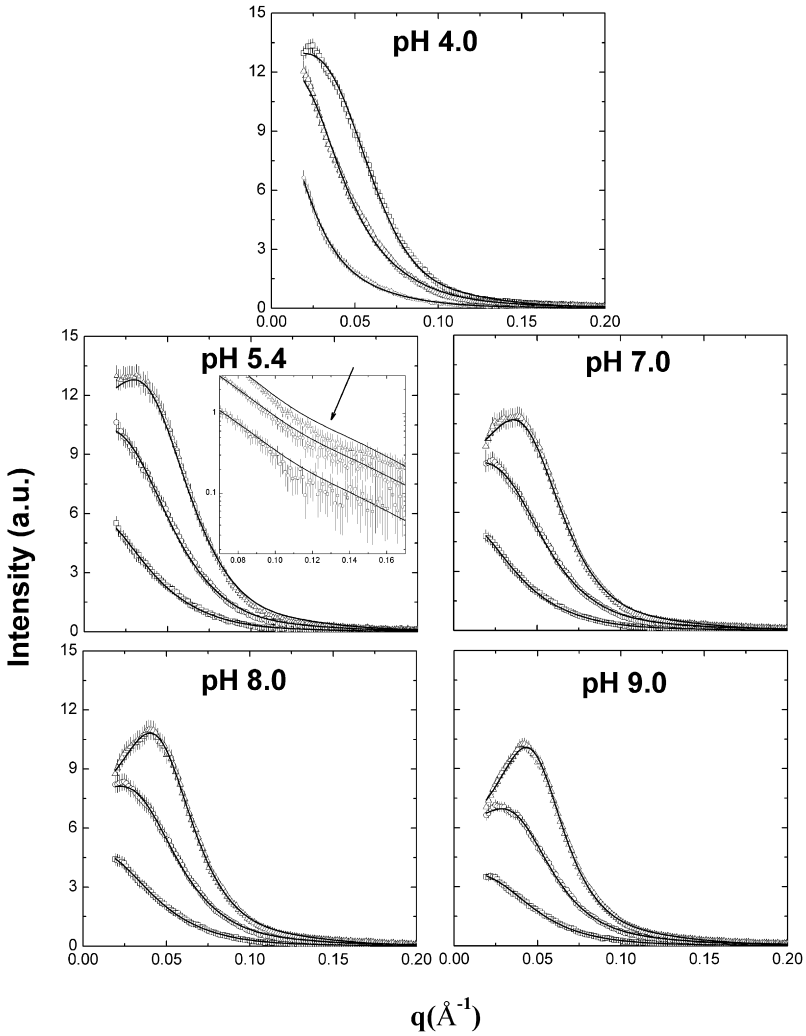

FIGURE 2 SAXS curves of the systems composed of BSA at 10 (*open squares*), 25 (*open circles*), and 50 (*open triangles*) mg/mL at pH 4.0, up to 9.0, along with the best fittings (*solid lines*). Adjustment parameters are described in Table 1. (*Inset*) Monolog plot of BSA at pH 5.4.

and 50 mg/mL) within the Global Fitting procedure. Fitting curves are presented in Fig. 2. Figs. 3 and 4 show the $S(q)$ functions and $V_{pp}(r)$ potentials (Eq. 2), respectively, obtained from the fittings. Therefore, the fitting results (*solid lines* in Fig. 2) reproduce quite well the experimental data, showing that the BSA native structure is preserved from pH 4.0 to 9.0 up to 50 mg/mL concentration.

Noteworthy is that the interplay between the attractive and repulsive forces leads to an effective interaction potential $V_{pp}(r)$ that changes with pH and concentration, as seen in Fig. 4. The values of J systematically decrease as the protein concentration increases at the same pH. For instance, at pH 4.0 the obtained values of J for an absolute value of the net protein charge of 10(2) are 28(3), 10(2), and 5(1) k_BT for 10, 25, and 50 mg/mL, respectively. This results in an effective interaction potential at the contact $V_{pp}(\sigma_{eff})$ that is deeper for 10 mg/mL of BSA than for 25 mg/mL and 50 mg/mL (Fig. 4). Such modification of the attractive potential with concentration has been previously reported, but it is still a matter of debate (18). We speculate that, most probably, the repulsive potentials, in particular the excluded volume effects, are more pronounced for increasing concentration and dominate the resulting effective interaction potential V_{pp}(r).

It should be remarked that only for the system composed of 10 mg/mL of BSA at pH 4.0, the resulting $V_{pp}(r)$ potential leads to a $S(q)$ function that has highest values for low q values (Fig. 3), characteristic of an attractive $S(q)$ function, justifying the excess of intensity $I(q)$ found in the corresponding SAXS curve (Figs. 1 and 2). At 10 mg/mL, the $S(q)$ function oscillates around the unity for pHs 5.4 and 7.0 (Fig. 3) and shows a small variation at low q values for pH 8.0 and 9.0, indicating that in such cases, the effective $V_{pp}(r)$ potential is not significantly affecting the scattering curves. On the other hand, for 25 mg/mL at neutral and basic pHs, the effectives values of $V_{pp}(r)$ and, hence, $S(q)$ functions (Figs. 3 and 4), start to be important over the SAXS curves at low q values, becoming pronounced for 50 mg/mL of BSA (Figs. 1 and 2).

Regarding the absolute value of the net BSA charge, $|Z|$ (Table 1), it resulted as pH-dependent. At pHs 4.0, 5.4, and 7.0 these values were 10(2), 8(1), and 13(2), respectively. It is important to mention that there is no consensus

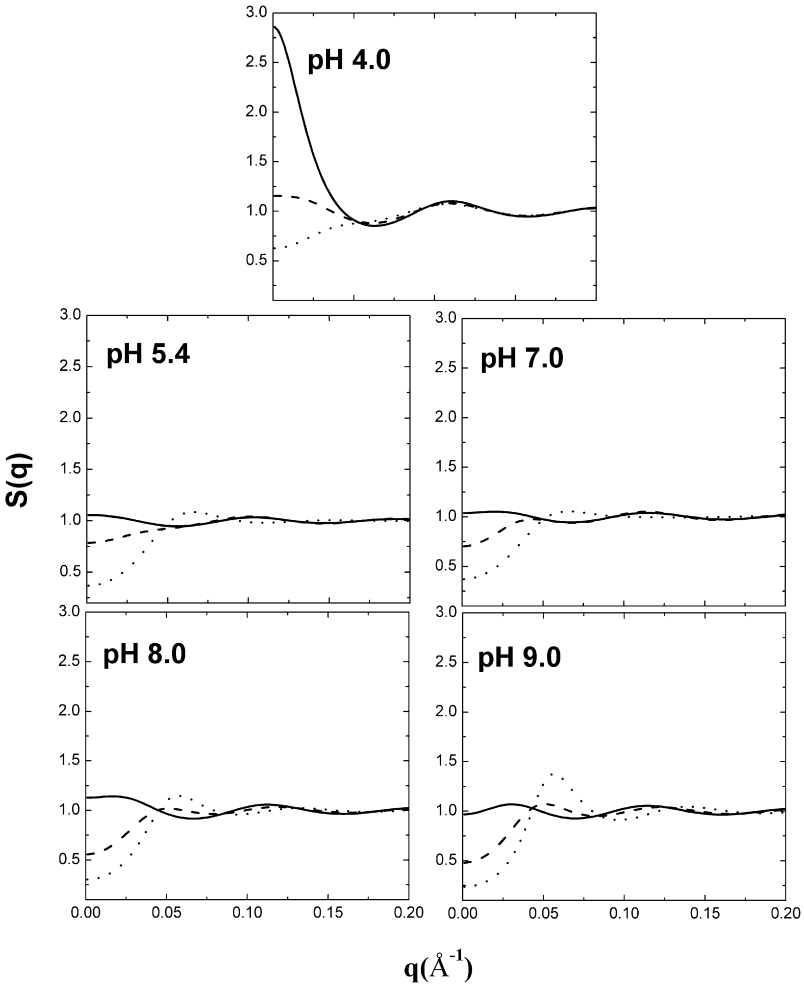

FIGURE 3 $S(q)$ functions obtained with the global fitting procedure; the parameters used to calculate these curves are described in Table 1. Solid, dashed, and dotted lines represent the $S(q)$ functions relative to $c_{BSA} = 10$, 25, and 50 mg/mL, respectively. Uncertainties in fitting parameters lead to <5% change in the amplitude of $S(q)$ function.

about the correct isoelectric point of BSA in the literature. However, this value should reside in the 4.8–5.6 interval (6,10). Thus, at pH 4.0 the net charge of the protein is positive, whereas at pH 7.0 is negative. In a pioneer work, Tanford and Buzzel (10) studied the net charge of BSA under different values of pH. The authors showed that at pH 5.0 and 7.3 BSA has a negative net charge of −4 and −13, respectively, in agreement with our results. It is interesting that, even at pH 5.4 that is near the BSA's pI, the protein shows some residual charge (Table 1). We evidenced that the values of J and $|Z|$ have a slightly different tendency at pH 5.4, in comparison to the other studied pHs (Table 1), probably because the system is near its pI. Interestingly, the model fails to fit well the SAXS data of the system composed of BSA at pH 5.4 and 50 mg/mL (*arrow* in the *inset* of Fig. 2) for large q range, even increasing the value of $|Z|$ from 8 to 13e at this concentration (Table 1). This point will be better explored later in the text.

Furthermore, at alkaline pH values (8.0 and 9.0), the effective protein-protein interaction potentials are more pronounced. This is due to an increase of the absolute value of the net protein charge as the pH increases ($|Z|$ doubles with respect to pH 7.0, whereas J changes to a lesser extent). Tanford and Buzzel (10) reported on the protein net charge at pH 8.5 and 9.3 as −20 and −22, respectively. In our case, we found $|Z|$ values of 20(2) and 26(2) for pH 8.0 and 9.0, respectively, in agreement with the mentioned work. Leonard et al. (17) studied the optical rotatory dispersion behavior of BSA (at 0.15 mg/mL) at neutral and alkaline pHs and evidenced that BSA suffers a shape transition between pHs 8.0 and 9.0. This is called the N-B transition and the B-form is characterized by a loosening structure (probably in the N-terminal region) and a small increase in the effective surface area: from 39,000 Å^2 to 47,000 Å^2 (6), as compared to the normal (i.e., N-form) one. We did not observe any conformational change by increasing pH up to 9.0 at higher BSA concentrations.

Zhang et al. (18) studied the effect of ionic strength (from 0–2 M of NaCl) and concentration (from 2–500 mg/mL), on BSA interaction potential at pH 7.0. In comparison to our approach, the authors adopted a different methodology to deal with the attractive interaction potential: for instance, they did not observe any influence of an attractive interaction over the SAXS curves from ionic strength that was equal to

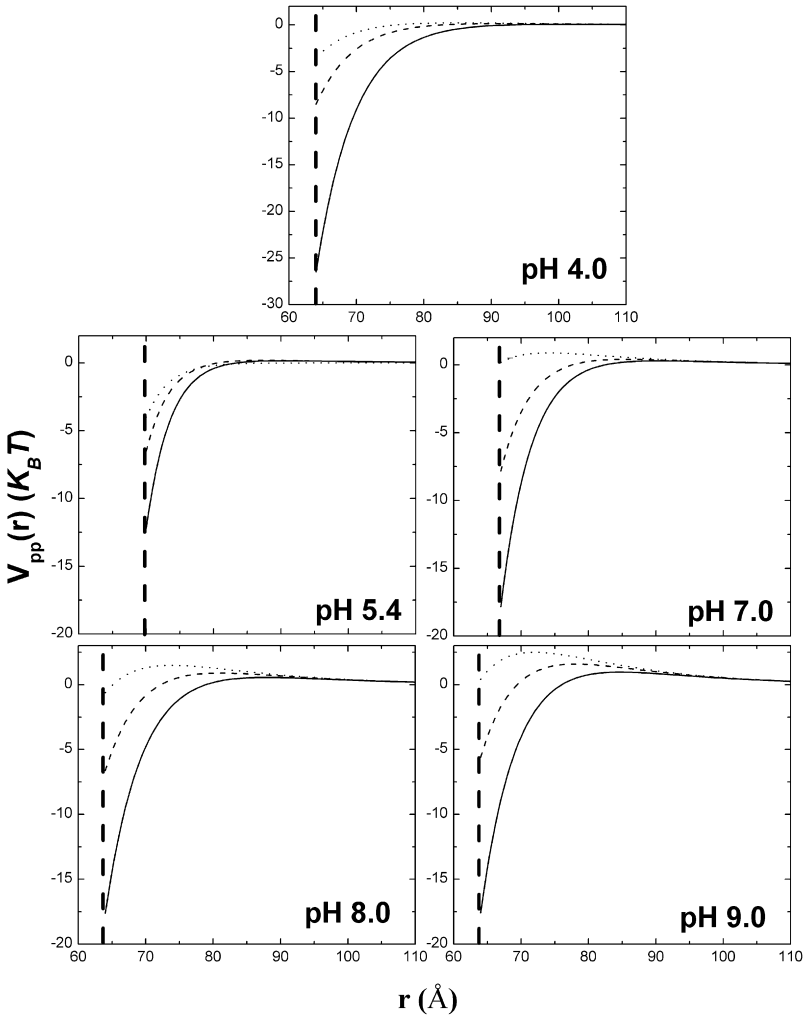

FIGURE 4 Protein-protein interaction potential, $V_{pp}(r)$ (Eqs. 2–5), for BSA at 10 (*solid line*), 25 (*dashed line*), and 50 (*dotted line*) mg/mL. Vertical dashed lines represent the protein effective diameter, σ_{eff}.

0 up to 300 mM of NaCl; and when necessary and for NaCl concentrations > 300 mM, they treated such attractive potential as square potential with small intensity (always $<1.5\,k_BT$) and long-range (varying from 7% up to 150% of the protein diameter, σ_{eff}). In any event, for the parameters related with the repulsive protein-protein interactions, Zhang et al. (18) found that, at pH 7.0 and low ionic strength (up to 300 mM), there are ~10–13 charges on BSA surface and the protein diameter is defined as 66.8 Å, calculated with the second virial coefficient—which is the same as our own findings.

Further, Sinibaldi et al. (20) used the same methodology employed in this article to study the influence of small amounts of urea on the BSA hydration shell. The authors demonstrated that in the absence of urea, at pH 7.0, there are ~16(2) charges and the value of d was fixed at 12(1) Å. However, the values of J were 14(2), 12(2), 10(2), and 8(2) k_BT, for 25, 50, 100, and 125 mg/mL, respectively. The values related with the repulsive potential from Sinibaldi's group are in agreement with those reported here. The parameters related to the attractive potential, however, are slightly different from those presented here. Nevertheless, it is important to mention that the buffer (and hence the ionic strength) employed in our work and that of Sinibaldi et al. (20) are different. Thus, it is possible that the differences shown in the attractive potential are from differences in the sample composition.

It is also important to stress that perception of the influence of attractive and repulsive potentials over the SAXS curves of the aqueous solutions containing 10 mg/mL of BSA was only possible due to the Global Fitting analysis. This is probably the major advantage of the Global Fitting procedure: to be able to obtain some information from the SAXS curves that could not be possible to evaluate in a single-SAXS curve data analysis. For instance, the SAXS curve of BSA 10 mg/mL at pH 5.4 has been previously described just by the protein form factor (11,13). However, as we demonstrated in this work, the influence of $V_{pp}(r)$, and hence $S(q)$, on the corresponding SAXS curve at pH 5.4 and 7.0, is small (Figs. 3 and 4). Therefore, BSA solutions containing 10 mg/mL at pH 5.4 and 7.0 are generally described in the literature as noninteracting protein systems (48).

BSA 50 mg/mL at pH 5.4

As previously mentioned, by considering $P(q)$ function as that corresponding to the protein crystallographic structure, our modeling fails to reproduce the scattering data for large q values for solutions containing 50 mg/mL of BSA (*inset* of Fig. 2, pH 5.4). To better investigate this mismatch, we decided to perform some simulations of the protein form factor for $q > 0.06$ Å^{-1} (i.e., in a q range where the $S(q)$ contribution can be negligible) using the effective oblate ellipsoidal model (18). Then, we first analyzed the SAXS curve of 10 mg/mL BSA at pH 5.4 comparing two different models (Fig. 5 *A*): the protein crystallographic structure and an effective oblate ellipsoid. As one can see in Fig. 5 *A*, both models reproduce well the SAXS intensity of BSA (10 mg/mL) at pH 5.4 in the whole q range within the experimental error bars, with the semiaxes of the effective oblate ellipsoid equal to 48 × 36 × 13 Å, corresponding to a volume of 94 × 10^3 Å^3. Such a volume is in good agreement with that calculated with the protein crystallographic structure (~92 × 10^3 Å). This is important information as the scattering particle volume (in our case the protein volume) must be constant if the protein does not aggregate.

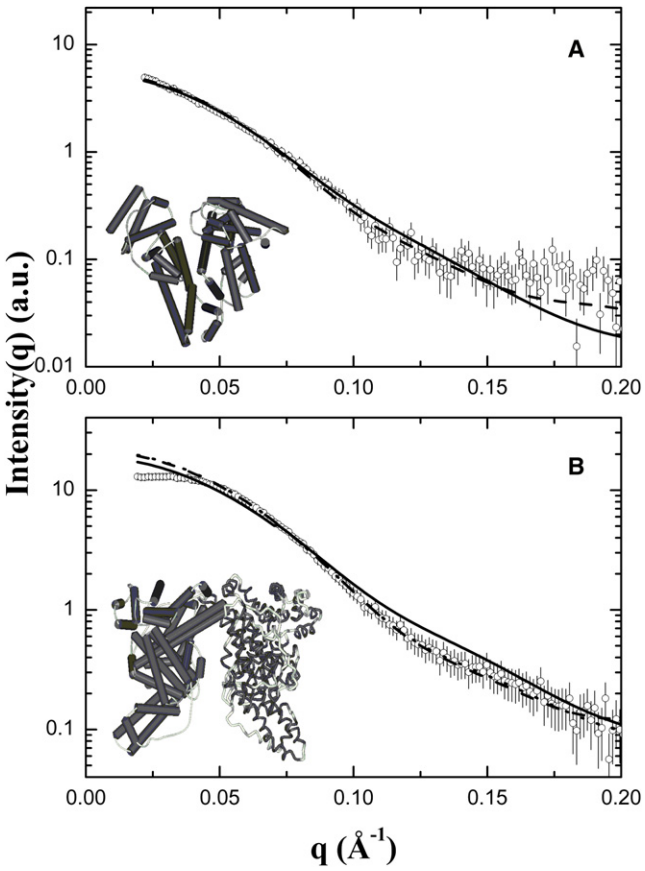

FIGURE 5 SAXS curves of BSA, 10 (*A*) and 50 (*B*) mg/mL, at pH 5.4. (*A*) Solid and dashed lines are the best $P(q)$ fit obtained with the HSA crystallographic structure (*inset*, PDB entry 1N5U) and the effective oblate ellipsoid model, respectively. (*B*) Solid line represents the best $P(q)$ fit obtained with HSA crystallographic structure, whereas the dashed and dotted lines represent the best $P(q)$ fit obtained with an effective ellipsoid and two-ellipsoid combination, respectively (see text for details). (*Inset*) Crystallographic structure of HSA dimer, proposed by Sugio et al. (46).

Fig. 5 *B* shows the SAXS curve of BSA, 50 mg/mL, at pH 5.4. As one can note, the model that uses the HSA crystallographic structure fails to reproduce the SAXS curve in the 0.10–0.15 Å^{-1} range. However, an effective oblate ellipsoid with semiaxes equal to 42 × 40 × 19 Å, and volume equal to 134 × 10^3 Å^3 (~40% larger than that calculated from the crystallographic structure), better-reproduces the SAXS data. Further, these values are in agreement with those reported for BSA at pH 7.0: 42 × 42 × 17 Å (18) (with a volume of 126 × 10^3 Å^3, ~36% larger than that of the crystallographic volume). Nevertheless, as far as we know, there is no physical reason for a protein volume enlargement (~30–40%) without protein aggregation. In the majority of the small-angle scattering studies dealing with BSA, small attention has been paid to the protein volume, even though this parameter is important in the SAXS data analysis.

An increase in the effective oblate ellipsoid volume is indicative of the presence of at least two different scattering volumes in the solution. Therefore, we also applied a model to the scattering curve in such a way that two distinct ellipsoids were taken into account: one representing BSA monomer, and the other, a dimer. The volumes of both ellipsoids were fixed as the volume of the monomer (94 × 10^3 Å^3) and the dimer (188 × 10^3 Å^3). In other words, this model supposes that there is a coexistence of monomers and dimers in solution and the SAXS data is, indeed, the contribution of these two populations. The presence of both monomers and dimers in solution could be responsible to the increase in the effective ellipsoid volume, as shown above. Using this methodology, the SAXS curve was well fitted with a mixture of scattering volumes representing the monomer and the dimer with semiaxes equal to 48 × 36 × 13 Å (the same parameters obtained for BSA 10 mg/mL at pH 5.4, Fig. 5 *A*) and 47 × 37 × 22 Å (with volume equals to 188 × 10^3 Å^3), respectively. It is interesting to notice that the semiaxes values suggest that BSA has a stacking on *c*-direction, when the values of semiaxes *a* and *b* are similar for both monomer and dimer. Noteworthy, Sugio et al. (46) reported one crystallographic structure for HSA, in which there is a dimer in the unit cell. In such a configuration, HSA molecules have a back-to-back relative position into this dimer (*inset* of Fig. 5 *B*). The structural parameters obtained for the dimer in the ellipsoidal model (47 × 37 × 22 Å) are in accordance with the relative position of HSA in the crystallographic structure. The use of the two-ellipsoid model also allows for calculating the percentage of protein in the monomer and dimer forms. In the case of BSA, at pH 5.4 and 50 mg/mL, these values were ~60% and 40% for monomer and dimer, respectively.

This methodology was also applied to all systems composed of 50 mg/mL of BSA (once this protein enlargement was not evidenced at 10 and 25 mg/mL at any pH).

At acidic, neutral, and basic pHs the amount of protein in the monomeric form exceeds 85%. Thus, in these cases the small amount of protein in the dimeric form did not contribute significantly to the SAXS curves. The decrease of the dimeric species, when the pH differs from the BSA's pI, must be attributed to the increase in the protein net charge and, as a consequence, in the repulsive electrostatic effects (see also Table 1), avoiding the aggregation. The possibility of having trimers, tetramers or other oligomers was not taken into account on this methodology. Another interesting point to mention is the calculation of the $S(q)$ function for the system composed of 50 mg/mL of BSA at pH 5.4. (In this case, it would be necessary to also take into account the monomer-monomer, the dimer-dimer, and the monomer-dimer interactions; however, such exploration is beyond the scope of this article.)

BSA at pH 2.0

The SAXS curves of BSA at pH 2.0 showed different profiles as compared to the SAXS curves of BSA at higher pH values. First of all, at pH 2.0 and 10 mg/mL, a peak at $q \approx 0.025$ Å^{-1} takes place over the scattering curve; this is due to the strong protein-protein interactions.

The study of partially or completely unfolded proteins is a very difficult task, once the protein shape is no longer generally distinct in itself but is, instead, composed of a collection of conformations (37). This can become even more complicated if interference effects between proteins occur over the SAXS curves. To try to overcome this problem, we apply a model to analyze the SAXS data for partially unfolded proteins taking also into account the protein-protein interaction. This model supposes that the protein form factor $P(q)$ can be described by the Pedersen and Schurtenberger model (35), and the interference effects, in a very crude approximation, are treated as a random phase approximation (29), as described in Eqs. 2–5, above.

It follows that Fig. 6 *A* shows the SAXS curve of BSA, 10 mg/mL, at pH 2.0 with the best calculated fitting curve. It should be stressed that the protein volume was fixed at 92×10^3 Å^3 (equal to the volume calculated with the protein crystallographic structure), as explained earlier in the text. Regarding the structural parameters, the contour length L, the Kuhn length b, and the protein inner cross-sections radius R were 168(10), 86(4), and 26(3) Å, respectively. These values indicate that BSA is partially unfolded, once it is well known that its maximum dimension is ~100 Å in the native conformation (11,13).

Concerning the parameters related to the interference effects, the protein effective diameter (σ_{eff}) and the absolute value of its net charge ($|Z|$) were 100(5) Å and 16(2), respectively, whereas the values of J and d were 17(1) k_BT and 5.8(5) Å, respectively. In addition, it should be remarked that these parameters have to be considered as effective values, because as free parameters they are certainly suppressing the deficiencies of this methodology.

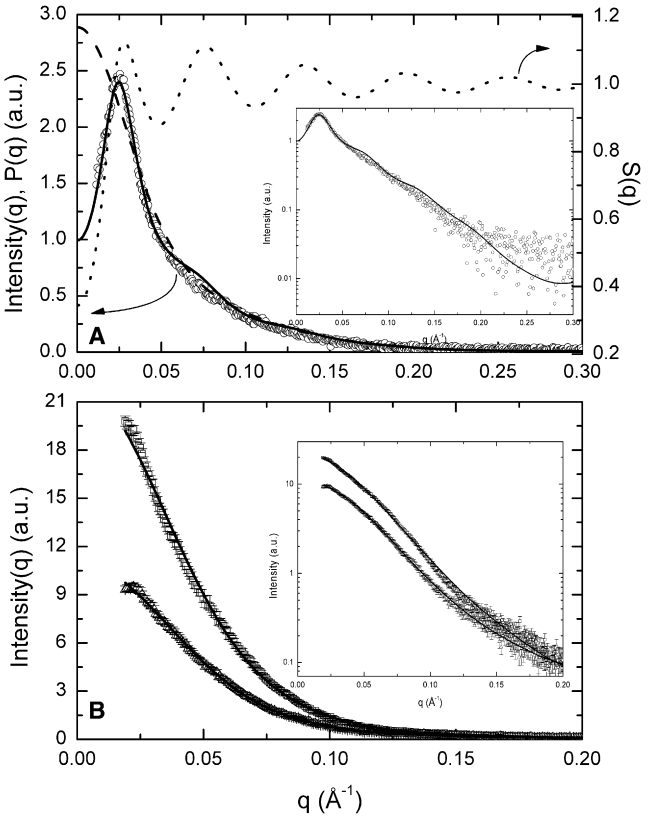

FIGURE 6 (*A*) SAXS curve of BSA at pH 2.0 and 10 mg/mL (*circles*). Dashed and dotted lines represent the form factor, $P(q)$, and the structure factor, $S(q)$, respectively, whereas the solid line is their product (Eq. 1). The same plot in the log-linear scale can be appreciated in the inset. (*B*) SAXS curves of BSA 25 (*triangles*) and 50 (*squares*) mg/mL at pH 2.0. Solid lines represent the best fittings obtained with the effective oblate ellipsoid model. The same plot in the log-linear scale can be appreciated in the inset.

Considering the concentration as 10 mg/mL ($n_p = 9.1 \times 10^{-8}$ Å^{-3}), it is possible to calculate the protein-protein (center-to-center) mean distance as

$$\overline{d} = 2\left(\frac{3}{4\pi n_p}\right)^{1/3}.$$

In this case, $\overline{d} \approx 280$ Å, ~110 Å bigger than the protein maximum dimension (in our case equal to 168(10)Å).

Interestingly, at 25 and 50 mg/mL, BSA seems to undergo to a more globular conformation, as compared with 10 mg/mL. However, this cannot be understood as a protein refolding, once the overall shape is different from that of the protein crystallographic structure. In these cases, we employed the effective oblate ellipsoid for the $P(q)$ model to analyze the SAXS data. (The interference effects were not taken into account, once they are no longer pronounced over the SAXS curves.) By employing this model in this way, Fig. 6 *B* shows the SAXS curves of BSA (25 and 50 mg/mL) at pH 2.0, along with the modeling. As one can see in the figure, the theoretical model reproduces well the SAXS data where the semiaxes of this ellipsoid are equal to 59, 35, and

14 Å, corresponding to a volume that is 25% bigger than that of the native BSA.

Kumar et al. (15) evidenced, by means of circular dichroism, that in diluted condition (1–2 μM, around ~0.1 mg/mL), HSA exists as a molten-globule state at pH 2.0. This state is considered as an intermediate state in the protein unfolding pathway. It is structurally characterized by a partially folded conformation that has its secondary structure nearly unaltered, but changes the tertiary one. Thus, at pH 2.0 at 25 and 50 mg/mL BSA, our results are indicating that BSA behaves as a molten-globule, as previously reported on HSA at low concentration regime. Furthermore, because of its dependence on concentration, once we could not observe it at 10 mg/mL, we speculated that the appearance of this molten-globule state could be related to some cooperative effect (likely from the effects of crowding).

It is well known that BSA undergoes conformational changes as the pH of the environment changes. At pH 4.0 the protein is in the F-form (Fast-migrating), which is characterized by an increase of the protein maximum dimension and a higher asymmetry (6), as compared to the N-form (the native or Normal one). Aoki and Foster (47), using electrophoresis, studied the behavior of BSA at 2 mg/mL at pH 2.0 up to 4.5. The authors demonstrated that BSA unfolds under such conditions and that this process has intermediate states in the pH 3.0 region. Noteworthy also is that, at pH 2.7, BSA undergoes another conformation change, reaching the E-form (Extended), which is characterized by an increase in the protein maximum dimension and asymmetry (6). In this work, the transition at pH 4.0 was not found, probably because of the high protein concentration employed here. The E-transition, however, was evidenced at 10 mg/mL (at pH 2.0) and it was characterized by an increase in the protein maximum dimension. As the concentration increases this form is changed, giving rise to a globular shape (at 25 and 50 mg/mL) that could be associated to a molten-globule state.

CONCLUSIONS

In this work, by means of the SAXS technique, we have studied the combined effect of concentration and pH variation on BSA tertiary structure. We have shown that BSA keeps its structure unaltered at pH 4.0 up to 9.0, in all three concentrations used (10, 25, and 50 mg/mL) without undergoing any significant conformational change. We have also demonstrated the coexistence of dimers and monomers in solution at pH 5.4 and 50 mg/mL, which amounted to 40 and 60%, respectively, and the predominance of monomers for pH 4.0, pH neutral, and pH basic. The decrease of the dimer amount with pH variation is due to an increase on the BSA charge, as the pH changes from 5.4 (Table 1). Further, our results support the conclusion that the delicate balance between the attractive and repulsive forces in the system inhibits extensive morphological changes as well as aggregation, at large amounts of protein.

At pH 2.0, BSA is partially unfolded at 10 mg/mL, changing to a more globular configuration upon increasing concentration, likely reaching a molten-globule state. Therefore, BSA at physiological concentrations (at ~35–43 mg/mL) keeps its native structure in neutral and basic environments, but it can change to a molten-globule state at pH 2.0 (i.e., unlike its behavior at low concentrations (6)). So, we may infer that the BSA conformational stability in the blood plasma can be attributable not only to its 17-disulfide bridges, which confer a significant stability to the protein structure, but also to the interaction potential inherent to the system at physiological conditions.

SUPPORTING MATERIAL

Two figures are available at http://www.biophysj.org/biophysj/supplemental/S0006-3495(09)01570-7.

We thank the National Laboratory of Synchrotron Light (Elettra, Trieste, Italy) for the use of their facilities.

This work was supported by research grants from Fundação de Amparo à Pesquisa do Estado de São Paulo and Concelho Nacional de Desenvolvimento Científico e Tecnológico (Brazil) to R.I. and Coordenação de Aperfeiçoamento a Pessoal de Nível Superior (Brazil) for a PhD fellowship to L.R.S.B.

REFERENCES

1. Guo, J., N. Harn, …, C. R. Middaugh. 2006. Stability of helix-rich proteins at high concentrations. *Biochemistry*. 45:8686–8696.
2. Ross, P. D., and A. P. Minton. 1977. Analysis of non-ideal behavior in concentrated hemoglobin solutions. *J. Mol. Biol.* 112:437–452.
3. Chiti, F., and C. M. Dobson. 1996. Protein misfolding, functional amyloid, and human disease. *Annu. Rev. Biochem.* 75:333–366.
4. Piazza, R. 2004. Protein interactions and association: an open challenge for colloid science. *Curr. Opin. Colloid Interface Sci.* 8:515–522.
5. Delaye, M., and A. Tardieu. 1983. Short-range order of crystalline proteins accounts for eye lens transparency. *Nature*. 302:415–417.
6. Peters, Jr., T. 1996. All About Albumins: Biochemistry, Genetics and Medical Applications. Academic Press, San Diego, CA.
7. Carter, D. C., and J. X. Ho. 1994. Structure of serum albumin. *Adv. Protein Chem.* 45:153–203.
8. Carter, D. C., B. Chang, …, Z. Krishnasami. 1994. Preliminary crystallographic studies of four crystal forms of serum albumin. *Eur. J. Biochem.* 226:1049–1052.
9. Curry, S., H. Mandelkow, …, N. Franks. 1998. Crystal structure of human serum albumin complexed with fatty acid reveals an asymmetric distribution of binding sites. *Nat. Struct. Biol.* 5:827–835.
10. Tanford, C., and J. G. Buzzel. 1956. The viscosity of aqueous solutions of bovine serum albumin between pH 4.3 and 10.5. *J. Phys. Chem.* 60:225–231.
11. Itri, R., W. Caetano, …, M. S. Baptista. 2004. Effect of urea on bovine serum albumin in aqueous and reverse micelle environments investigated by small angle x-ray scattering, fluorescence and circular dichroism. *Braz. J. Phys.* 34:55–63.
12. Ferrer, M. L., R. Duchowicz, …, A. U. Acuña. 2001. The conformation of serum albumin in solution: a combined phosphorescence depolarization-hydrodynamic modeling study. *Biophys. J.* 80:2422–2430.
13. Santos, S. F., D. Zanette, …, R. Itri. 2003. A systematic study of bovine serum albumin (BSA) and sodium dodecyl sulfate (SDS) interactions by

electrical conductivity, surface tension and SAXS. *J. Colloid Interface Sci.* 262:400–408.

14. Michnik, A., K. Michalik, and Z. Drzazga. 2005. Stability of bovine serum albumin at different pH. *J. Therm. Anal. Calorim.* 80:399–406.
15. Kumar, Y., S. Tayyab, and S. Muzammil. 2004. Molten-globule like partially folded states of human serum albumin induced by fluoro and alkyl alcohols at low pH. *Arch. Biochem. Biophys.* 426:3–10.
16. Christensen, H., and R. H. Pain. 1991. Molten globule intermediates and protein folding. *Eur. Biophys. J.* 19:221–229.
17. Leonard, Jr., W. J., K. K. Vijai, and J. F. Foster. 1963. A structural transformation in bovine and human plasma albumins in alkaline solution as revealed by rotatory dispersion studies. *J. Biol. Chem.* 238: 1984–1988.
18. Zhang, F., M. W. A. Skoda, …, F. J. Schreiber. 2007. Protein interactions studied by SAXS: effect of ionic strength and protein concentration for BSA in aqueous solutions. *Phys. Chem. B.* 111:251–259.
19. Spinozzi, F. http://www.isf.univpm.it/biophysics/software.htm.
20. Sinibaldi, R., M. G. Ortore, …, P. Mariani. 2007. Preferential hydration of lysozyme in water/glycerol mixtures: A SANS study. *J. Chem. Phys.* 126:235101.
21. Sinibaldi, R., M. G. Ortore, …, P. Mariani. 2008. SANS/SAXS study of the BSA solvation properties in aqueous urea solutions via a global fit approach. *Eur. Biophys. J.* 37:673–681.
22. Guinier, A., and G. Fournet. 1955. Small Angle Scattering of X-Rays. Wiley, New York.
23. Fegin, L. A., and D. I. Svergun. 1987. Structure Analysis by Small Angle X-Ray and Neutron Scattering. Plenum Press, New York.
24. Spinozzi, F., D. Gazzillo, …, F. Carsughi. 2002. Interaction of proteins in solution from small-angle scattering: a perturbative approach. *Biophys. J.* 82:2165–2175.
25. Ortore, M. G., F. Spinozzi, …, D. Russo. 2009. Combining structure and dynamics: non-denaturing high-pressure effect on lysozyme in solution. *J. R. Soc. Interface.* 6:S619–S634.
26. Wardell, M., Z. Wang, …, D. C. Carter. 2002. The atomic structure of human methemalbumin at 1.9 Å. *Biochem. Biophys. Res. Commun.* 291:813–819.
27. Spinozzi, F., F. Carsughi, …, L. Q. Amaral. 2000. SAS from inhomogeneous particles with more than one domain of scattering density, arbitrary shape. *J. Appl. Cryst.* 33:556–559.
28. Svergun, D. I., S. Richard, …, G. Zaccai. 1998. Protein hydration in solution: experimental observation by x-ray and neutron scattering. *Proc. Natl. Acad. Sci. USA.* 95:2267–2272.
29. Hansen, P., and I. R. McDonald. 1976. Theory of Simple Liquids. Academic Press, London, UK.
30. Kelkar, V. K., J. Narayanan, and C. Manohar. 1992. Colloidal dispersions: use of exact potentials approximation. *Langmuir.* 8:2210–2214.
31. Narayanan, J., and X. Y. Liu. 2003. Protein interactions in undersaturated and supersaturated solutions: a study using light and x-ray scattering. *Biophys. J.* 84:523–532.
32. Tardieu, A., A. Le Verge, …, L. Belloni. 1999. Proteins in solution: from x-ray scattering intensities to interaction potentials. *J. Cryst. Growth.* 196:193–203.
33. Velev, O. D., E. W. Kaler, and A. M. Lenhoff. 1997. Protein interactions in solution characterized by light and neutron scattering: comparison of lysozyme and chymotrypsinogen. *Biophys. J.* 75:2682–2697.
34. Curtis, R. A., J. M. Prausnitz, and H. W. Blanch. 1998. Protein-protein and protein-salt interactions in aqueous protein solutions containing concentrated electrolytes. *Biotechnol. Bioeng.* 57:11–21.
35. Pedersen, J. S., and P. Schurtenberger. 1996. Scattering functions of semi-flexible polymers with and without excluded volume effects. *Macromolecules.* 29:7602–7612.
36. Kratky, O., and G. Porod. 1949. X-ray studies of string-like molecules in solution. *Rec. Trav. Chim. Pays-Bas.* 68:1106–1123.
37. Cinelli, S., F. Spinozzi, …, P. Mariani. 2001. Structural characterization of the pH-denatured states of ferricytochrome-*c* by synchrotron small angle x-ray scattering. *Biophys. J.* 81:3522–3533.
38. Mariani, P., F. Carsughi, …, C. M. Bergamini. 2000. Ligand-induced conformational changes in tissue transglutaminase: Monte Carlo analysis of small-angle scattering data. *Biophys. J.* 78:3240–3251.
39. Ortore, M. G., R. Sinibaldi, …, P. Mariani. 2008. New insights into urea action on proteins: a SANS study of the lysozyme case. *J. Phys. Chem. B.* 112:12881–12887.
40. Press, W. H., S. A. Teukolsky, …, B. P. Flannery. 1994. Numerical Recipes. The Art of Scientific Computing. Cambridge University Press, Cambridge, U.K.
41. Shukla, A., E. Mylonas, …, D. I. Svergun. 2008. Absence of equilibrium cluster phase in concentrated lysozyme solutions. *Proc. Natl. Acad. Sci. USA.* 105:5075–5080.
42. Bendedouch, D., and S. H. Chen. 1983. Structure and interparticle interaction of bovine serum albumin in solution studied by small-angle neutron scattering. *J. Phys. Chem.* 87:1473–1477.
43. Nossal, R., C. J. Glinka, and S. H. Chen. 1986. SANS studies of concentrated protein solutions. I. Bovine serum albumin. *Biopolymers.* 25:1157–1175.
44. Chodankar, S., V. K. Aswal, …, A. G. Wagh. 2008. Small-angle neutron scattering study of structural evolution of different phases in protein solution. *Phys. Rev. E Stat. Nonlin. Soft Matter Phys.* 77:031901.
45. Lee, C. T., K. A. Smith, and T. A. Hatton. 2005. Photocontrol of protein folding: the interaction of photosensitive surfactants with bovine serum albumin. *Biochemistry.* 44:524–536.
46. Sugio, S., A. Kashima, …, K. Kobayashi. 1999. Crystal structure of human serum albumin at 2.5 Å resolution. *Protein Eng.* 12:439–446.
47. Aoki, K., and J. Foster. 1957. Electrophoretic behavior of bovine plasma albumin at low pH. *J. Am. Chem. Soc.* 79:3385–3393.
48. Tjioe, E., and W. T. Heller. 2007. ORNL_SAS: Software for calculation of small-angle scattering intensities of proteins and protein complexes. *J. Appl. Cryst.* 40:782–785.